

Diversity-induced synchronized oscillations in close-to-threshold excitable cells arranged on regular networks: effects of network topology

I. Vragovic,¹ E. Louis,¹ C. Degli Esposti Boschi,² and G. J. Ortega^{3,†}

¹Departamento de Física Aplicada, Instituto Universitario de Materiales and Unidad Asociada CSIC-UA, Universidad de Alicante, E-03080 Alicante, Spain

²Unità di Ricerca INFN di Bologna, viale Berti-Pichat 6/2, 40127, Bologna, Italia

³Departamento de Física, F.C.E.N. Universidad de Buenos Aires and CONICET, Pabellón I, Ciudad Universitaria, 1428, Capital Federal, Argentine

(Dated: February 16, 2019)

The question of how network topology influences emergent synchronized oscillations in excitable media is addressed. Coupled Van der Pol-FitzHugh-Nagumo oscillators arranged either on regular rings or on a square lattice are investigated. Clustered and declustered rings are constructed to have the same number of next-nearest-neighbors (four) and a number of links twice that of nodes. The system is chosen to be close-to-threshold, allowing bursting to be triggered by a weak diversity. The results clearly illustrate the crucial role played by network topology. In particular we found that network performance (bursting and synchronization) is mainly determined by the network average path length and by the standard deviation of path lengths. The shorter the average path length and the smaller the standard deviation, the better the network performance. Local properties, as characterized by the clustering coefficient, are less important.

PACS numbers: 05.45.Xt, 87.18.Sn, 89.75.-k

I. INTRODUCTION

During the last decade, a considerable attention has been drawn to identify the mechanisms that may induce global oscillatory behavior in excitable media [1, 2, 3, 4, 5, 6, 7, 8, 9, 10, 11]. In particular, a great effort has been devoted to investigate the effects of heterogeneity in networks of a variety of oscillators of biological interest [1, 2, 3, 4, 5, 6, 7, 8]. It has been shown that diversity may induce bursting in an otherwise non-oscillating medium, and, for large enough coupling between the network elements, oscillations may become synchronized. In a recent work we showed that if the system is close-to-threshold, synchronized oscillations may be induced by an arbitrarily weak diversity [12]. In our opinion this result is relevant for living systems to the extent that is natural to assume an inherent weak diversity in the composition of a biological aggregate at some level.

The present work is addressed to investigate how network topology may affect global oscillations. Although modifying the cluster topology in the way we do here may not be of particular significance in the case of pancreatic cells, the example addressed by Cartwright's model [5] and consequently in our analysis [12], identifying the key characteristics of a particular network, as far as global synchronization is concerned, is of general interest. In addition we investigate the dynamic behavior of these systems trying to identify the mechanisms that trigger and sustain synchronized oscillations.

The paper is organized as follows. In the subsection

IIA we discuss the main features of the coupled van der Pol-FitzHugh-Nagumo equations outlining the main reasons why diversity may trigger bursting. The measures we use to quantify the degree of bursting and synchronization are described in subsection IIB. The networks investigated in this work are described in subsection IIC as well as the two quantities used to characterize local and global structure, namely, the average path length and the clustering coefficient. The results are described and discussed in Section III. We discuss how bursting and synchronization vary with the coupling between the elements in the network and the effects of the spatial distribution of heterogeneity (diverse cells or elements in the network) remarking on the differences between networks. Moreover, we consider the dependence of global oscillations on the size of the system and on the network topology. Finally the question of how synchronized oscillations are sustained is addressed. The achievements of our research are summarized in Sec. IV.

II. MODEL AND METHODS

A. Van der Pol-FitzHugh-Nagumo equations

We describe the excitable medium by means of a system of coupled van der Pol-FitzHugh-Nagumo equations [13, 14, 15, 16], arranged on a network. Each oscillator is assumed to represent a cell in a living system. The set of equations is written as, [5, 12]:

$$\frac{dy_i}{dt} = z_i - y_i^3 + y_i + Q_i \quad (1)$$

† Electronic address: desposti@bo.infn.it

‡ Electronic address: ortega@df.uba.ar

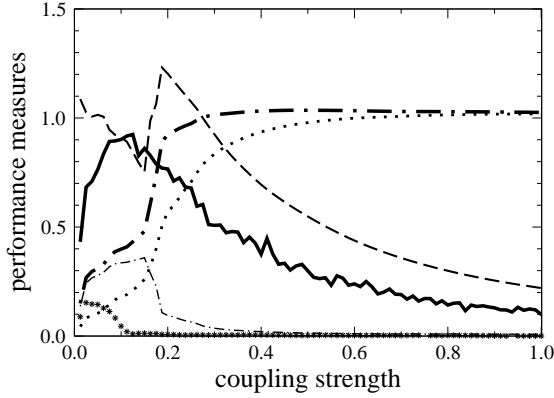


FIG. 1: Bursting intensity and synchronization versus strength of coupling between excitable cells described by Eqs.(1) and (2). Cells are arranged on a square network of linear size $l=10$, with 98 continuously active sites ($\alpha=0.61$) and 2 silent impurities ($\beta=0.61$). The results are averaged over 10 different realizations of impurity distributions. Cell bursting intensity (I^{CB}) -thick dot-dashed line. Intensity of bursting of the whole network (I^{NB}) -dotted. Synchronization (S): with respect to an ordinary (full), or an impurity cell (dashed). Dispersion of cell bursting intensities (D^{BI}) - thin dot-dashed, and of the period of oscillations (D^P) - stars (see text).

$$\frac{dz_i}{dt} = \gamma_i + \alpha_i + z_i: \quad (2)$$

Like all relaxation oscillators, FitzH ough-N agum o oscillator has a variable y_i with a fast release and a variable z_i with a slow accrual phase. These variables correspond to the potential across the nonlinear resistance (cell membrane) and the current through the supply, respectively. Parameters α and β describe the (membrane) resistance and the square root of the ratio inductance/capacitance respectively. The strength of coupling between nearest-neighbors is denoted by Q [17], while the function that describes coupling Q_i is given by,

$$Q_i = \sum_{j=1}^{k_i} (y_j - y_i) = \sum_{j=1}^N L_{ij} y_j; \quad (3)$$

where k_i is the number of nearest-neighbors (or connectivity) of cell i , and N is the total number of cells in the network. L_{ij} is usually referred to as the Laplacian matrix, whose structure plays an essential role in determining the behavior of the network, as it contains all the information on network's topology; for instance it has been used to investigate the stability of the synchronized state once established [18].

In the absence of coupling (isolated cell) the parameter α , which is proportional to the charging potential of the cellular membrane, determines the behavior of the

oscillator. If α is outside the oscillating range ($\alpha > \alpha_c$, being the threshold), the cell is in stable equilibrium. It is called an excitable cell and can be either silent ($\alpha < \alpha_c$) or continuously active ($\alpha > \alpha_c$). Otherwise, the equilibrium is unstable ($\alpha < \alpha_c$) and the cell performs oscillations along a limit cycle. The threshold is given by:

$$\alpha_c = \frac{P}{2} \frac{3^2 + 2^2}{3^3} \quad (4)$$

and for the chosen set of parameters $P=2$ and $\beta=0.5$, kept constant hereafter in this work, it takes the value 0.60412.

The coupled FitzH ough-N agum o equations were solved on several regular networks with N nodes, $2N$ links and a connectivity $k_i=4$ for all nodes. All cells were assumed to be active with $\alpha_i = \alpha$, but a small fraction x of them, called impurities, that were taken to be silent with $\alpha_i = \beta$, $i=1; \dots; [xN]$. The numerical results discussed in this work correspond to $\alpha=0.61$. Although for this parameter value no cell bursts when isolated, coupling and impurities may trigger oscillations. A simple way to visualize this effect is to consider the spatial average of

$$h_i = (1 - 2x): \quad (5)$$

This clearly shows that the presence of impurities may shift the effective parameter value below threshold, forcing an originally quiescent cell to oscillate. Although this expression can be used to estimate the fraction of impurities above which the oscillatory behavior emerges, it cannot account for the important differences in the performance of ordinary and impurity cells that can actually show up (see below). Fortunately, an effective parameter can be estimated separately for each cell [5]:

$$\alpha_i^{eff} = \alpha_i + \sum_{j=1}^{k_i} (y_j - y_i): \quad (6)$$

At quiescence there is no coupling between cells having the same parameter value. However, in the case of one silent ($\alpha_j = \beta$) and one continuously active cell ($\alpha_i = \alpha$) we can write $(y_j - y_i) = (\alpha_j - \alpha_i) = 2$. The coupling between different cells is therefore of crucial importance for the effective change of cells parameters. Let us call $m(x)$ the average number of the nearest-neighbors of opposite nature for ordinary (+) and impurity (-) cells. The effective parameter can then be written as:

$$\alpha_i^{eff} = [\alpha - 2m(x)]: \quad (7)$$

For large enough N , the average number of nearest neighbors $m(x)$ is given by,

$$m_+(x) = \sum_{n=1}^N \frac{x^n}{n} (1-x)^{4-n} = 4x; \quad (8)$$

$$m(x) = \sum_{n=1}^4 \binom{4}{n} x^n (1-x)^{4-n} = 4(1-x): \quad (9)$$

This indicates that, on average, impurities can be much more affected by coupling than ordinary cells. To get a grasp of the implications of this result, let us give some numbers. The critical fraction of impurities x_c required to force ordinary cells to burst can be derived from $x_c^{eff} = \dots$:

$$x_c = \frac{1}{8} (1 - \dots): \quad (10)$$

Taking a typical value for the coupling strength $\dots = 1$ and the values of the other two parameters given above, we obtain $x_c = 0.0024$. The effective parameter of the impurity cell for this value of x is $x_c^{eff} = 1.8$. The effect is so strong that the parameter has not only changed its sign, but it is also well outside the bursting regime. This result underlies the differences in the behavior of ordinary and impurity cells discussed below.

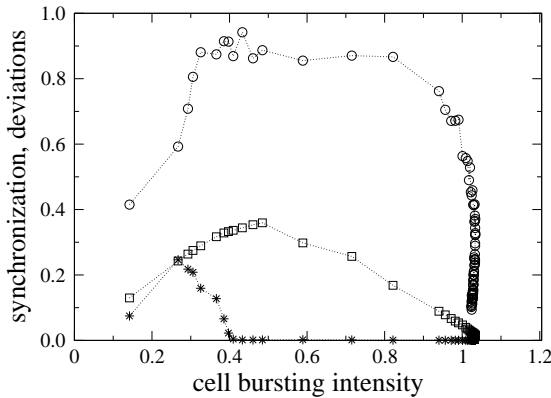


FIG. 2: Synchronization (circle) and dispersion of bursting intensities (square) and periods of oscillations (stars) versus cell bursting intensity. Cells were arranged on the square lattice with $N = 100$. The percentage of impurities is 2%, while coupling strength is varied over the range $\dots \in (0;1)$. See also caption of Fig. 1.

B. Measures of bursting intensity and synchronization

We can quantify the emergence of oscillatory behavior by calculating the average bursting intensity of individual cells or of the network as a whole, over a sufficiently long time interval. As discussed elsewhere [12] transient periods can be quite long for uncoupled cells, while in the case of strongly coupled cells the coherent oscillatory behavior is almost instantaneously attained (cp. Fig.

1 in Ref. [12]). In order to minimize the contribution of transient periods for weakly coupled cells and attain time-independent statistics [12], the averages are computed starting from a large initial time t_i after which the stationary state is reached for any coupling regime, and over a time interval $t = t_f - t_i$ long enough to cover a sufficient number of periods. In a typical case the dynamic equations were solved with an integration step of 0.05, taking averages from $t_i = 100$ up to $t_f = 200$. For the values of cell parameters given above, the intrinsic period is around $T = 10$, so that bursting intensity was averaged over approximately 10 periods.

We use as a measure of cell bursting intensity (CBI) at cell j , the standard deviation:

$$CBI_j = \sqrt{\frac{1}{t} \sum_{t=t_i}^{t_f} y_j^2(t) - \langle y_j \rangle^2}; \quad (11)$$

where $\langle y_j \rangle = \frac{1}{t} \sum_{t=t_i}^{t_f} y_j(t)$ is the time average over interval t . A high value of CBI_j implies a large amplitude of cell oscillations around its time average, while a low value would reveal an almost non-oscillatory behavior.

We also define the average of the cell bursting intensity over the whole network as:

$$CBI = \frac{1}{N} \sum_{j=1}^N CBI_j; \quad (12)$$

Depending on the neighborhood, the effective parameters x_j^{eff} can largely differ from cell to cell (see preceding subsection), inducing different bursting intensities. The dispersion of cells bursting intensity with respect to its network average can be quantified by means of the standard deviation:

$$DBI = \sqrt{\frac{1}{N-1} \sum_{j=1}^N (CBI_j)^2 - (CBI)^2}; \quad (13)$$

Synchronization is evaluated by comparing the current phases of each oscillator with the current phase of a randomly chosen reference cell (ordinary or impurity), and calculating the time average over the interval t :

$$s = \sqrt{\frac{1}{(N-1)t} \sum_{j \neq r, t=t_i}^{t_f} [\cos \phi_j(t) - \cos \phi_r(t)]^2}; \quad (14)$$

Shifting all the limit cycles to have a common center we define $\cos \phi_j(t) = y_j(t) - r_j(t) = \tilde{y}_j(t) = \frac{y_j(t) + z_j(t)}{2}$, $y_j(t) = y_j(t) - h_j(t)$ and $z_j(t) = z_j(t) - h_j(t)$. The sum in s is not extended to all possible reference sites in order to limit the computational time. The smaller s the better the synchronization. The measure chosen to

test synchronization in this work is more demanding than those used in previous works, in the sense that, there, only differences in a single dynamic variable were evaluated [5, 12]. Note, however, that in calculating the phase used in Eq. (14) average values were subtracted from each dynamical variable. This means that this measure does not account for possible differences in those averages. Anyhow this is not essential as far as the evaluation of global oscillatory behavior is concerned.

In order to improve synchronization, first the majority of cells should be oscillating with the same frequency. Once that is achieved, dephasing between cells should vanish. Thus, an essential parameter for characterizing the emergence of synchronization is the dispersion of oscillating periods; we quantify this dispersion by means of the standard deviation divided by the average period $T = \frac{1}{N} \sum_{i=1}^N T(i)$:

$$D.P. = \frac{1}{T} \sqrt{\frac{1}{N} \sum_{i=1}^N \frac{T(i)^2}{T^2}}; \quad (15)$$

Finally, we can measure the bursting intensity of the network as a whole comparing the time dependent network bursting amplitude with its temporal average over the interval t [19].

$$N.B.I. = \sqrt{\frac{1}{t} \sum_{t_i}^t \frac{X^2}{[y(t)^2 - \langle y \rangle^2]}}; \quad (16)$$

with $\langle y \rangle = \frac{1}{N} \sum_{i=1}^N y_i(t)$ the average network amplitude $y(t) = \frac{1}{N} \sum_{i=1}^N y_i(t)$ and its temporal average $\langle y \rangle = \frac{1}{t} \sum_{t_i}^t y(t)$. In order to have large values of $N.B.I.$, the majority of cells must be both bursting and synchronized. Thus, the network bursting intensity $N.B.I.$ is an appropriate quantity for the simultaneous measure of both bursting and synchronization in excitable media [19].

C. Networks

As the main aim of this work is to investigate the role of topology, we shall compare the results obtained on various regular networks having a number of links twice that of nodes, and the same degree (number of nearest neighbors). We choose the square lattice with periodic boundary conditions (this guarantees that all nodes i have degree $k_i = 4$) and two types of regular rings. The first one is the simplest clustered regular lattice, which consists of a ring with additional connections to the next-nearest neighbors (this is usually referred to as $K = 2$). The second type of ring has zero clustering (see below) and is constructed as follows. Standard (clustered) rings with $K = n$ are built by linking each site to all neighbors

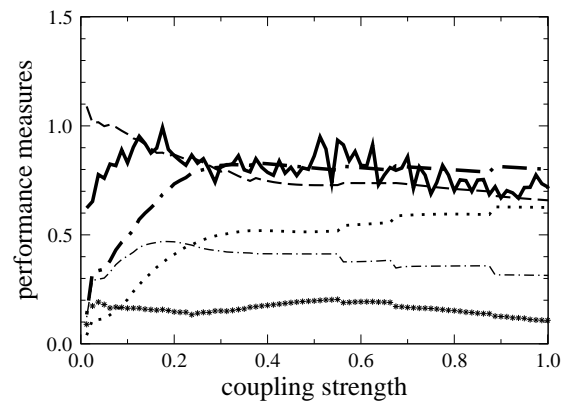
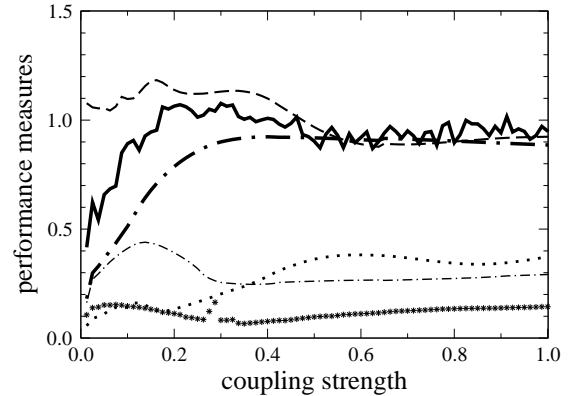


FIG. 3: Same as Fig. 1 for clustered (upper) and declustered (lower) rings both with $N = 100$ nodes.

from the first up to the n -th. Declustered rings, denoted as $K = n$, have additional links only to the n -th neighbors. In this work we shall investigate ring networks with $K = 2$ and $K = 3$; both have degree $k_i = 4$ for all nodes.

The topology of connections between sites can strongly influence the cooperation and the exchange of information between them. The structural properties of a graph are usually quantified by the average path length L and the clustering coefficient C [20, 21]. The average path length is calculated as the network average of the shortest graph distances between two nodes for all possible pairs,

$$L = \frac{1}{N(N-1)} \sum_{i \neq j} d_{ij}; \quad (17)$$

The clustering coefficient C measures to which extent are the neighbors of each site connected to each other. It is defined as follows,

$$C = \frac{1}{N} \sum_i \sum_{j \neq k} \frac{n_{jk}}{k_i(k_i-1)}; \quad (18)$$

where j and k are nearest-neighbors of i and $n_{jk} = 1$ only

if there is a link between j and k . This definition does only give $C \neq 0$ if there are triangles in the network. This is the case of clustered rings such as that chosen here ($K = 2$) but it is not that of the square lattice nor that of the declustered ring, both having $C = 0$.

The average length for the three networks investigated here can be calculated analytically. The result for the clustered ring is,

$$L(K = 2) = \frac{N}{4} \frac{N-2+1}{N-1}; \quad (19)$$

valid only for $N = 4n$, where n is an integer. For very large systems this behaves as $L \sim N^{-1}$. In the case of the declustered ring we obtain,

$$L(K = 3) = \frac{N}{6} \frac{N-2+4}{N-1}; \quad (20)$$

valid only for networks with a number of nodes $N = 6n$, n being an integer. In this case the limit for $N \rightarrow \infty$ is $L \sim N^{-1}$.

It is interesting to write a general formula for an arbitrary K in the case of a declustered ring,

$$L(K) = \frac{N}{2K} \frac{N-2+(K-1)}{N-1}; \quad (21)$$

where $i=1,2$ for K odd or even, respectively. This formula is valid for $N = 2Kn$, where n is an integer.

Finally, the result for the square lattice with periodic boundary conditions is,

$$L(\text{square}) = \frac{N^{3/2}}{2(N-1)}; \quad (22)$$

its asymptotic behavior being $L \sim 0.5 \sqrt{N}$.

The main difference between rings (clustered or declustered) and the square lattice is that the latter is far smaller than the former as its average length increases sublinearly with the network size. It is worth trying to understand why the square lattice behaves in this way in terms of the structure of the Laplacian matrix. By appropriately renumbering sites, any square lattice with periodic boundary conditions can be mapped into a ring in which additional links are introduced between: $\frac{N}{p}$ nodes and their $(\frac{N}{p}-1)$ th and $(\frac{N}{p}+1)$ th neighbors, $\frac{N}{p}$ nodes and their $(\frac{N}{p}-1)$ th and $(\frac{N}{p}+1)$ th neighbors; the remaining $N-2\frac{N}{p}$ being additionally connected to their $(\frac{N}{p}-1)$ th and $(\frac{N}{p}+1)$ th neighbors. For large N this is equivalent to a declustered ring with $K = \frac{N}{p}$. In fact Eq. (21) for declustered rings gives, for $K = \frac{N}{p}$, the same asymptotic behavior than Eq. (22) the square lattice. In addition, contrary to regular rings with $K = 2$ or $K = 3$, where additional links introduce non-zero elements in the second and third subdiagonals of the Laplacian matrix, respectively (being short-range for any system size), in the square lattice the additional links are long-ranged and introduce non-zero elements in the $(\frac{N}{p}-1)$ th and $(\frac{N}{p}+1)$ th subdiagonals.

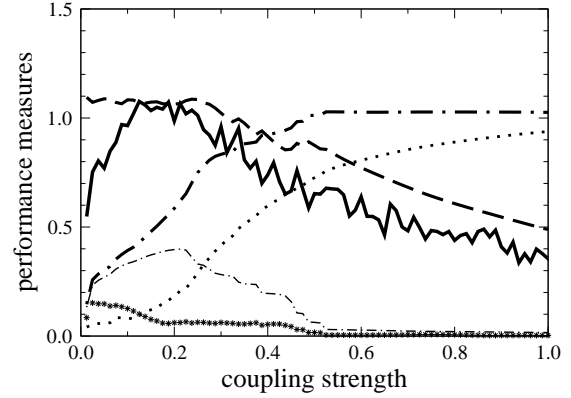


FIG. 4: Same as Fig. 1 for the square lattice of linear size $l = 18$ with 6 impurities.

III. RESULTS

A. Coupling Strength

The analysis of the influence of coupling between cells on bursting intensity and synchronization reveals two different regimes (see Fig. 1). The results correspond to a square lattice having $N = 100$ nodes with a fraction of impurities $x = 0.02$. At weak coupling (< 0.2), the perturbation originating from impurity cells is not spread much over the network. Ordinary cells are only weakly impelled to oscillate, but with different amplitudes. The dispersion around the average bursting intensity of cells is large, reaching its maximum for 0.15 , cp. Fig. 1. Furthermore, the finite dispersion of the oscillating periods for < 0.1 indicates that cells excited to various bursting levels oscillate with different frequencies, which is the main reason for low synchronization in this coupling regime. In addition, such a weak coupling is not strong enough to eliminate large dephasings between cells oscillating with the same frequency. Consequently, the bursting of the network as a whole is much weaker than the bursting of individual cells, as synchronization is still not attained.

In the strong coupling regime (> 0.8), oscillations of individual cells become more intense and synchronization is improved, leading to a strong bursting of the network as a whole. Cells are strongly oscillating and there are no significant differences in frequencies (the dispersion of oscillating periods is practically zero). Increasing the coupling strength further, gradually eliminates phase differences and synchronization is improved. Finally, ordinary cells are much better synchronized with each other, while the impurity cells are forced to oscillate in the same way as the rest of the network only in the case of very strong coupling, cp. Fig. 1. Reasons for the different behavior of ordinary and impurity cells were given in subsection II A.

The aforementioned mechanism of improving synchronization is even more evident if we plot bursting intensity, network synchronization, and dispersion of intensities and period of oscillations in a single graph (Fig. 2). Synchronization is the worst when the deviation of period reaches its maximum for cells bursting intensity around 0.3. After that, it is practically unchanged until all cells oscillate with the largest amplitude. Approaching the maximum bursting level, the dispersion of intensities decreases, and synchronization is rapidly improved by eliminating differences in phase of the oscillators.

In the case of rings, synchronization is not obtained even for strong coupling, cf. Fig. 3. The large average path length of the clustered ring ($L = 12.88$ to be compared with $L = 5.05$ for square lattice of the same size), hinders the effective spread of perturbations coming from impurity cells. Both the dispersion of bursting intensities and the dispersion of oscillating periods remain large. Similar results are obtained for declustered rings, with a modest improvement of δ . Bursting intensity and synchronization are again quite low, due to the large average path length ($L = 9.09$). This indicates that collective oscillatory behavior is determined mainly by the average length of the network, and not by its local properties quantified by the clustering coefficient. In particular note the highly different performances of the square network and the declustered ring, both having zero clustering and appreciably different average path lengths: the shorter the length the better the performance.

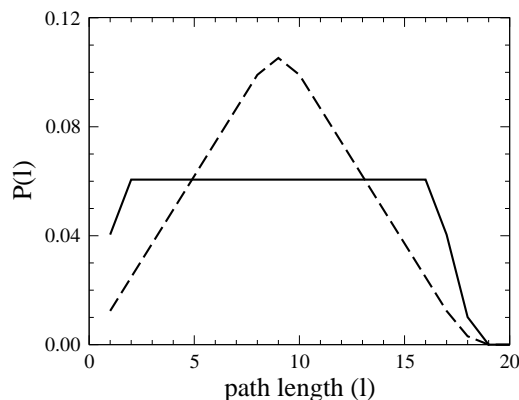


FIG. 5: Probability density function of path lengths in a declustered ring with $N = 100$ nodes and $K = 3$ (continuous line) and in the square lattice with $N = 18^2$ nodes (broken line).

The question now is whether the average path length is or not the only topological feature that matters. We address this question analyzing a square lattice of a bigger size (18×18 , with $N = 324$), having almost the same characteristic length ($L = 9.03$) as a declustered ring with $K = 3$ and 100 sites (see above). The coupling strengths are varied over the same range ($\beta \in (0;1)$), while the

fraction of impurities is not changed ($x = 0.02$ as above). As shown in Fig. 4 performance is now much better than that found for the declustered ring (see Fig. 3) indicating that the average length is not enough to characterize network behavior. Fig. 5 shows the probability density function of path lengths in the two networks. We note that while this density shows a well defined peak at the average path length in the case of the square lattice, it is almost constant in the declustered ring. As a consequence the standard deviation of path lengths is appreciably smaller in the former (3.7 to be compared with 4.9 for the declustered ring). We believe that the different standard deviations of path lengths is the origin of the noticeably different performance of the two networks. Besides, this result suggests that homogeneous systems (as far as path lengths are concerned) are more efficient in triggering bursting and synchronization.

B. Distance between impurity cells

All the results presented up to now are averaged over several realizations of impurity distribution. It turns out that the oscillating behavior strongly depends on the distance between impurity cells. It is likely that, increasing the distance between them, would improve bursting and synchronization, as the overlapping of the domains of their influences is decreased. In other words, the average path length from ordinary sites to the closest impurities becomes shorter. This is illustrated in Fig. 6 where synchronization is plotted as a function of the distance between impurities. Rings and square lattices behave in a similar way (the pace at which synchronization improves with distance is similar in all networks) although as already pointed out synchronization is much poorer in the former.

C. The Size of the Network

We have investigated how synchronization varies with the network size in the case of the square lattice. Calculations were carried out keeping the fraction of impurities constant $x = 0.02$. As argued in [8] the effective coupling constant varies with the average network length as $l = L^2$. This can be easily checked by noting that in the continuum limit the coupling term of Eq. (3) behaves as,

$$Q / \frac{\partial^2 y}{\partial x^2}; \quad 0 < x < L; \quad (23)$$

Then, rescaling the spatial variable to bring to evidence size effects we find,

$$Q / \frac{1}{L^2} \frac{\partial^2 y}{\partial x^2}; \quad 0 < x < 1; \quad (24)$$

where L should be interpreted as the average linear size of the system. In order to check this behavior we have

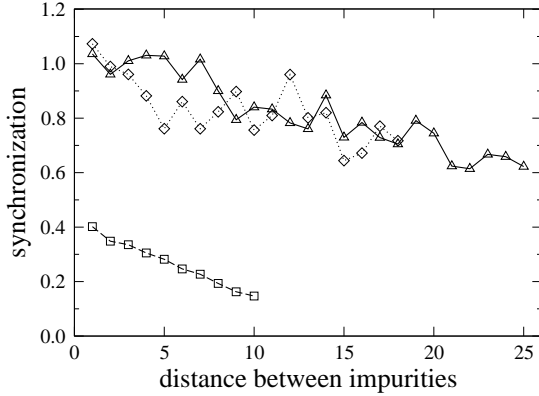


FIG. 6: Synchronization (ordinary reference site) versus distance between the two impurity cells. Cells were arranged on different networks of size $N = 100$: square network (square), clustered (triangle) and declustered (diamond) rings. Coupling strength and fraction of impurities are $\gamma = 0.5$ and $x = 0.02$, respectively.

carried out calculations with a coupling strength either constant ($\gamma = 0.5$) or proportional to L^2 ($\gamma = 0.5N = 100$). The numerical results are depicted in Fig. 7. We first note that, for $\gamma = 0.5$, synchronization is gradually deteriorated as the size of the system increases. The pace at which it worsens is rather slow due to the sublinear behavior of the average path length (see above). Rescaling the coupling strength as just mentioned, gives a synchronization that remains almost unchanged as the size increases, proving the validity of the scaling argument. A similar analysis for circular networks shows a much faster worsening of the system performance when coupling is kept constant, again due to the fast (linear) increase of the average length with the network size. However, the scaling argument is still valid.

D. Sustaining synchronized oscillations

The results and discussion of the preceding subsections clearly show that coupling between cells and diversity are the main cause of synchronized oscillations in the systems under study. Coupling is finite only if y_i are not all identical. Then, how synchronization is sustained? Fig. 8 shows $y_i(t)$ and the coupling function $Q_i(t)$ for a single cell i as a function of time. The average over the whole network $\langle y(t) \rangle$ is also shown. The results correspond to the strong coupling regime ($\gamma = 0.5$). First we note that a characteristic oscillating pattern and coherent behavior is achieved almost instantaneously. Besides, this occurs for any initial condition. On the other hand no significant differences between time dependent bursting of a particular cell and network average are noted. The coupling function $Q_i(t)$ shows an oscillatory pattern similar to that of y_i , although it is an order of magnitude smaller.

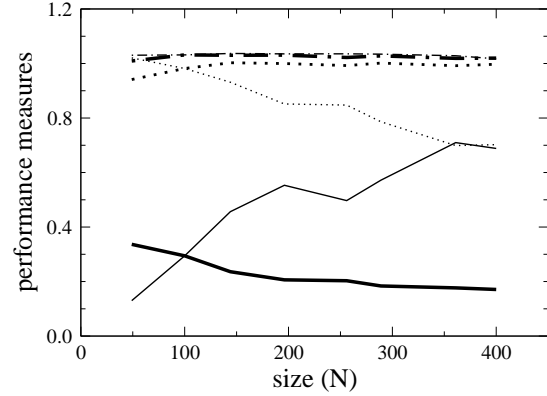


FIG. 7: Cell bursting intensity (dot-dashed line), network bursting intensity (dotted line) and synchronization with respect to an ordinary reference site (full line) versus size of square network. The coupling strength was taken either constant ($\gamma = 0.5$, thin lines) or proportional to the square of the average path length ($\gamma = 0.5N = 100$, thick lines).

This shows that a small difference between variables in each cell is enough to sustain synchronized oscillations. In addition the oscillatory pattern is stable: Any perturbation of phase coordinates (within the range of limit cycle) at time t_0 , could be viewed as setting new initial conditions for bursting starting at that time. The effect of the perturbation would then be eliminated after a few oscillations, restoring the characteristic pattern.

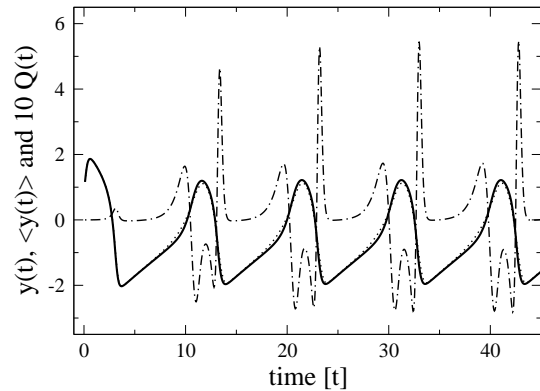


FIG. 8: Time dependence of bursting of a randomly chosen ordinary cell ($y_i(t)$ - full line), its coupling function ($10 Q_i(t)$ - dotted) and bursting averaged over the whole network ($\langle y(t) \rangle$ - dashed). Cells were arranged on a square lattice of linear size $l = 10$. The results correspond to a single realization of impurity distribution. The chosen coupling strength ($\gamma = 0.5$) is large enough to trigger synchronized oscillations.

IV. CONCLUSIONS

The conclusions that emerge from our investigation of the induction of global synchronized oscillations by diversity in excitable regular systems are:

1. Cells and network activity and synchronization, as collective phenomena, depend mainly on global properties of the network. Shortening the average path length by merely changing the topology, while keeping constant the number of sites and links, can activate and synchronize the network more easily. In addition we found that the standard deviation of the path length is also a very crucial variable: the smaller it is the better the network performance becomes.

2. Local properties quantified by the clustering coefficient do play a role much less significant than the average path length and its standard deviation.

3. Synchronization in the square lattice is improved by increasing the strength of coupling between the excitable cells. In the strong coupling regime most of the cells are highly activated, oscillating with the same frequencies and negligible dephasing.

4. Circular regular networks with short range links are hardly synchronized even when cells are strongly coupled, due to their long average path length and large standard deviation.

5. Bursting and synchronization depend on the spatial distribution of impurity cells, improving as the distance between those cells increases.

6. Finally, we have revisited the behavior of van der Pol-FitzHugh-Nagum excitable media when their size is varied. We found that the dynamical behavior of the network can be kept unchanged when the system size increases, provided that the coupling strength is increased proportionally to the average path length. Regarding synchronization, the optimal topologies are the ones for which this length increases more slowly with the system's size.

ACKNOWLEDGMENTS

Financial support by Fet Open Project COSIN IST-2001-33555 and the Universities of Barcelona and Alicante is gratefully acknowledged.

-
- [1] E. M. Eron, *Phys. Rep.* 218, 1 (1992).
- [2] P. Smolen, J. Rinzel and A. Sherman, *Biophys. J.* 64, 1668 (1993).
- [3] J. E. Truscott and J. Brindley, *Bull. Math. Biol.* 56, 981 (1994).
- [4] A. Sherman, *Bull. Math. Biol.* 56, 811 (1994).
- [5] Julian H. E. Cartwright, *Phys. Rev. E* 62, 1149 (2000).
- [6] B. Hu and C. Zhou, *Phys. Rev. E* 61, R1001 (2000).
- [7] G. De Vries and A. Sherman, *J. Theor. Biol.* 207, 513 (2000).
- [8] G. De Vries and A. Sherman, *Bull. Math. Biol.* 63, 371 (2001).
- [9] H. Hasegawa, *Phys. Rev. E* 67, 041903 (2003); *ibid* 70, 021912 (2004).
- [10] J. Aguirre, E. Mosekilde, and M. A. F. Sanjuan, *Phys. Rev. E* 69, 041910 (2004).
- [11] B. Lindner, J. Garcia-Ojalvo, A. Neiman, and L. Schimansky-Gier, *Phys. Rep.* 392, 321 (2004).
- [12] C. degli Esposti Boschi, E. Louis, G. Ortega, *Phys. Rev. E* 65, 012901 (2002).
- [13] B. van der Pol and J. van der Mark, *Philos. Mag.* 6, 763 (1928).
- [14] R. A. FitzHugh, *J. Gen. Physiol.* 43, 867 (1960).
- [15] R. A. FitzHugh, *Biophys. J.* 1, 445 (1961).
- [16] J. S. Nagumo, S. Arimoto, and S. Yoshizawa, *Proc. IRE* 50, 2061 (1962).
- [17] Eqs. (1) and (2) of Ref. [12] contain an errata: the coupling term appear in Eq. (2) instead of Eq. (1). However, all numerical results presented therein correspond to the correct writing of the equations shown in this work.
- [18] T. Nishikawa, A. E. Motter, Y. C. Lai, and F. C. Hoppensteadt, *Phys. Rev. Lett.* 91, 014101 (2003).
- [19] L. F. Lago-Fernandez, R. Huerta, F. Corbacho and J. A. Sigüenza, *Phys. Rev. Lett.* 84, 2758 (2000).
- [20] D. J. Watts and S. H. Strogatz, *Nature (London)* 393, 440 (1998).
- [21] R. Albert and A.-L. Barabasi, *Rev. Mod. Phys.* 74, 47 (2002).